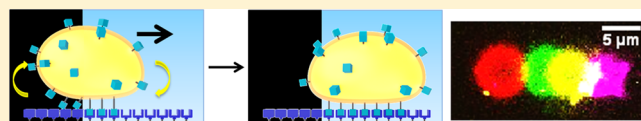# Light-Guided Motility of a Minimal Synthetic Cell

Solveig M. Bartelt,[†] Jan Steinkühler,[‡] Rumiana Dimova,[‡] and Seraphine V. Wegner*,[†]

[†]Max Planck Institute for Polymer Research, Ackermannweg 10, 55128 Mainz, Germany
[‡]Theory and Bio-Systems, Max Planck Institute of Colloids and Interfaces, Science Park Golm, 14424 Potsdam, Germany

Ⓢ *Supporting Information*

ABSTRACT: Cell motility is an important but complex process; as cells move, new adhesions form at the front and adhesions disassemble at the back. To replicate this dynamic and spatiotemporally controlled asymmetry of adhesions and achieve motility in a minimal synthetic cell, we controlled the adhesion of a model giant unilamellar vesicle (GUV) to the substrate with light. For this purpose, we immobilized the proteins iLID and Micro, which interact under blue light and dissociate from each other in the dark, on a substrate and a GUV, respectively. Under blue light, the protein interaction leads to adhesion of the vesicle to the substrate, which is reversible in the dark. The high spatiotemporal control provided by light, allowed partly illuminating the GUV and generating an asymmetry in adhesions. Consequently, the GUV moves into the illuminated area, a process that can be repeated over multiple cycles. Thus, our system reproduces the dynamic spatiotemporal distribution of adhesions and establishes mimetic motility of a synthetic cell.

KEYWORDS: Motility, optogenetics, GUV adhesion, synthetic cell, photoswitchable

Motility is a key feature of living cells and is at the core of complex life processes including immune response, development, and the progression of diseases.[1] Mammalian cell motility on a two-dimensional (2D) substrate is a complex multistep event that requires four synchronized steps: (1) formation of membrane protrusions, (2) new adhesions to the substrate at the leading edge, (3) contraction of the cell body, and (4) detachment at the trailing edge.[2] To orchestrate these processes the cell relies on a complex molecular machinery including the actin cytoskeleton to form protrusions, integrins, which mediate adhesion to the substrate, myosin-dependent contractions, and a multitude of other regulatory proteins to coordinate different steps. An additional layer of complexity is that in a moving cell the symmetry between the back and the front is broken and different events, which span different time and length scales, have to be spatiotemporally controlled and synchronized (Figure 1A).

To understand the underlying complexity of cell motility, minimal synthetic cells provide simplified models and give mechanistic insight into how different machinery contributes to the process.[3] Toward this goal different machinery required for cell motility to form cell protrusions, contraction and adhesion have been introduced in GUVs (giant unilamellar vesicles), which are frequently used as a cell-like compartment.[4] In GUVs, the polymerization of actin in the presence of motor proteins leads to the deformation of the vesicle, formation of membrane protrusions, and oscillatory motion of the vesicles.[5,6] Adding myosin and coupling the actomyosin network to the membrane generates tension and results in symmetry breaking during the contraction of the network but does not lead to GUV movement. Furthermore, the cell adhesion receptor, integrin, has been functionally incorporated into GUVs and can prompt adhesion to substrates functionalized with the adhesion peptide RGD and extracellular matrix

proteins.[7−11] Likewise, other interactions such as biotin–streptavidin,[12] E-cadherin,[13] lectin-sugar[14] and electrostatic interactions[15,16] were used to understand GUV adhesion to substrates. Despite all these studies, which provide great molecular insight into key players in cell motility, none of them have achieved the ultimate goal of replicating cell motility.

Part of the challenge in mimicking cell motility in a minimal synthetic cell is that in a migrating cell there is an asymmetry in terms of adhesion between the leading and the trailing edge. More and new adhesions form at the front to generate high traction forces coupled to the actin network and fewer adhesions at the back, which disassemble, enable the detachment, and retraction of the cell rear. Overall this asymmetry in adhesions is dynamically maintained and results in a directional cell movement. Replicating this dynamic spatiotemporal distribution of adhesions in a minimal synthetic cell requires a trigger that induces asymmetry in adhesions between the front and rear of a GUV and hinders the system to reach an equilibrium state. Such a trigger must provide spatial control at the sub GUV scale (typical diameter about 20 μm) and temporal control at a time scale that is relevant for a migrating cell (typical speed between 0.1 to 4 μm/min[17]). In addition, like in a cell these triggered adhesions must be reversible and have matching formation and reversion kinetics so that the trailing edge can detach as new adhesion are formed in the front. Current synthetic cell models based on integrins and synthetic interactions neither provide such spatiotemporal control nor the required reversibility and dynamics.
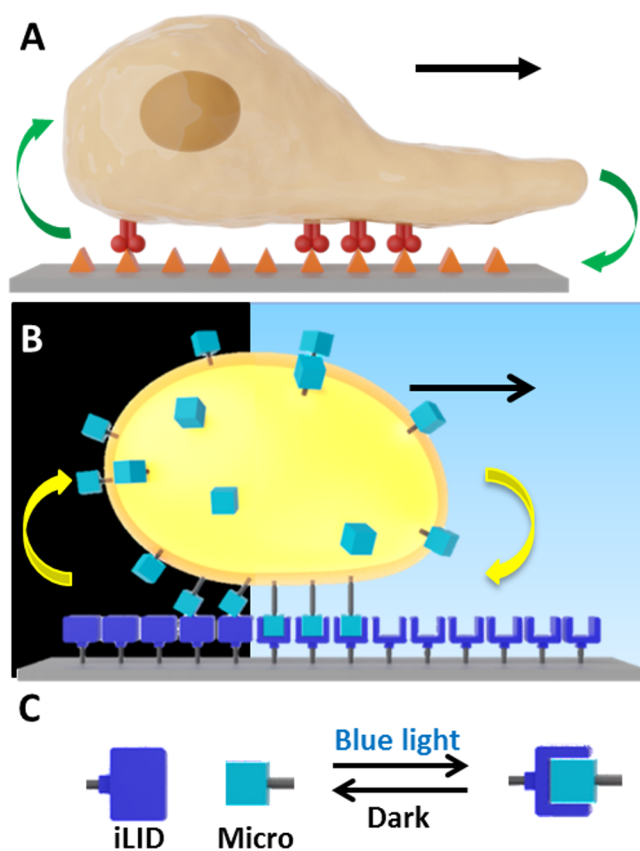
Figure 1. Cell vs GUV motility. (A) Simplified scheme of cell motility. Cell motility requires new adhesions to form at the leading edge, whereas adhesions have to disassemble at the trailing edge for the cell to move forward. The adhesion receptor integrin, is shown in red and the adhesion motif on the substrate in orange. (B) The light-controlled adhesion of a GUV allows to spatiotemporally control adhesions by partially illuminating the GUV. This mimics the dynamic asymmetry of adhesions in a minimal synthetic cell and leads to movement of the GUV. (C) The proteins iLID and Micro interact under blue light and dissociate in the dark.

To reproduce cell motility in a minimal synthetic cell and create dynamic asymmetry in adhesions, we established reversible GUV adhesions with high spatiotemporal control and matching on/off dynamics. For this aim, we propose to control the adhesion of GUVs to a substrate with visible light by using photoswitchable protein interactions as adhesion mediators (Figure 1B). Photoswitchable proteins provide reversible remote control at micrometer spatial resolution and down to second time scales with visible light.[18,19] Some photoswitchable protein interactions have already been used to control the interactions of mammalian and bacterial cells with substrates using light.[20,21] A critical parameter in selecting the photoswitchable protein interaction is that it has comparable on and off switching dynamics, so that the front and the rear of the GUV move at the same speed. In particular, we picked the photoswitchable protein iLID (improved light-induced dimer protein, based on the LOV2 domain), which binds to the protein Micro under blue light and dissociates from it in the dark (Figure 1C).[22] Our choice for this couple is based on the fact that the interaction between iLID and Micro reverses quickly in the dark within seconds to minutes, which matches the fast photoactivation with blue light. Other photoswitchable protein interactions like those between the PhyB and PIF6

under red light as well as CRY2 and CIBN or nMagHigh and pMagHigh under blue light activate much faster with light than they reverse in the dark.[20,21] The rapid deactivation of the PhyB/PIF interaction is possible with far-red light but is technically more complex as it would require the coillumination with a second far-red light source.

As the first step to establish photoswitchable adhesions, we immobilized His-tagged iLID as the adhesion ligand onto a polyethylene glycol (PEG)-coated glass substrate with Ni^{2+}-NTA end groups (Ni^{2+}-NTA end groups about 40 pmol/cm^2)[23] through the His-tag-Ni^{2+}-NTA interaction and His-tagged Micro as the adhesion receptor onto deflated GUVs (POPC + 10 mol% POPG + 0.1 mol % DGS-Ni^{2+}-NTA, Ni^{2+}-NTA end groups ca. 0.25 pmol/cm^2) including a lipid with a Ni^{2+}-NTA headgroup (Figure 2A). The GUVs were osmotically deflated by partially evaporating the outer buffer, leading to excess membrane allowing for membrane fluctuations and various vesicle morphologies including spherical-cap-like adhering states.[24] In addition, the GUVs were loaded with a solution (100 mM sucrose) of higher density compared to that of their surrounding so that they sunk onto the substrate. The vesicles were labeled with a red-shifted fluorescent dye (1,1′-dioctadecyl-3,3,3′,3′-tetramethylindodicarbocyanine) to observe them with confocal microscopy in x,z direction without activating the photoswitchable protein interaction. In the dark, Micro functionalized GUVs settled on the iLID functionalized substrate but did not exhibit significant adhesion, that is, the GUVs were free to displace by diffusion and convection and the weak membrane-substrate interactions were also witnessed by thermal membrane undulations in the vicinity of the substrate (Figure 2B, $t = 0$ min). Only upon activation of the iLID−Micro interaction with blue light (Laser at 488 nm), the GUVs adhered strongly to the substrate, as observed from the deformation of the GUV expressed in an increase in adhesion area and suppression of optically resolvable membrane fluctuations in the adhesion segment (Figure 1B, $t = 15$ min, Supporting Information, Figure S1). This adhesion was reversible in the dark. After turning off the blue light, the adhesion area decreased approximately to the initial dark state (Figure 2B, $t = 20$ min). The adhesion of the GUVs could be turned on and off repeatedly over four blue light/dark cycles (Supporting Information, Figure S2). Additional control experiments showed that the GUVs do not adhere to the iLID-functionalized substrate in the dark over time or if the GUVs were not functionalized with Micro (Supporting Information, Figure S3). Similarly, GUVs also adhered light-dependently if the position of the iLID and Micro proteins are swapped, that is, immobilizing iLID on the GUV and Micro on the substrate (Supporting Information, Figure S4). Nonetheless, in all following experiments we immobilized the light-activated protein partner iLID on the PEG-coated glass substrate, so that iLID is not mobile and its spatially controlled photoactivation is not wiped out by diffusion in the GUV membrane.

When the membrane stiffness of the GUVs was increased by adding cholesterol, the light-triggered GUV deformation was less pronounced, showing only reduced formation of an adhered membrane segment (20 mol % cholesterol) or adhered membrane segments that were below the optical resolution (40 mol % cholesterol) (Supporting Information, Figure S5). Likewise, when the GUVs were not osmotically deflated, the light-dependent GUV adhesions only led to minor deformation of the GUV (Supporting Information, Figure S6).
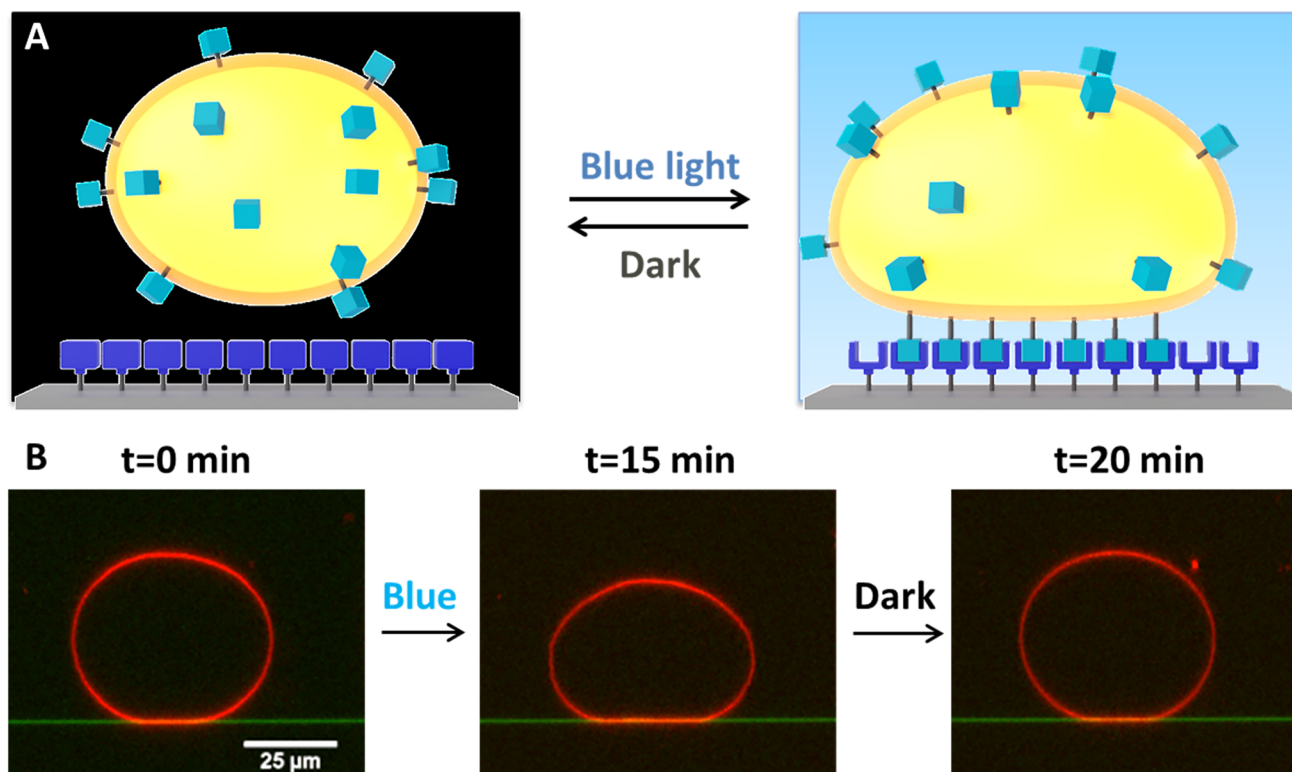
Figure 2. Light-dependent adhesion of a GUV to a substrate. (A) Light-dependent adhesion of a GUV decorated with Micro to a substrate functionalized with iLID. Upon light illumination the GUV adheres to the substrate and detaches in the dark. (B) Fluorescence microscopy images of a GUV over a time line being illuminated with blue light for 15 min adhered (compare first and second image). After further 5 min in the dark the GUV detached (last image). Micrographs represent (*x,z*) side-views. Red channel is membrane dye and green channel is the reflection of the 561 nm laser at the glass−water interface.

Hence, lower bending rigidity of the deflated GUVs is a critical requirement to observe light-dependent GUV deformation and membrane fluctuations to mimic the protrusions formed in migrating cell.

Kinetics of the light-induced adhesion and unbinding were quantified by time-resolved imaging and analysis of the GUV-substrate contact area (Figure 3A). The GUVs showed an increase of adhesion region to about double the size within the first 10 min of blue light illumination (Figure 3A, Light). Subsequently, when the GUVs were placed in the dark, the adhesion area of the GUVs decreased back to about its initial value within 5−6 min (Figure 3A Dark). However, the exact kinetics did vary between individual GUVs, presumably reflecting the complex relationship between membrane adhesion and iLID light activation, membrane dynamics, vesicle tension and size (Supporting Information, Figure S7). The fact that the adhesion under blue light and detachment in the dark take place at a similar and at minute time scale is important as the kinetics of attachment in the front and of detachment in the back of the GUV should match so that the cell can move in one piece. Notably, in a migrating cell adhesion and detachment also takes place on this time scale. When cells adhere, integrins enrich/cluster at the adhesion site and are depleted from other parts of the cell membrane. We used mOrange tagged Micro to observe whether Micro also enriched at the adhesion site upon photoactivation but could not detect significant Micro enrichment at the adhesion site (Supporting Information, Figure S8). It is also interesting that in some cases upon reversing GUV adhesion in the dark, excessive membrane shedding in the form of small vesicles

from the GUVs is observed (Supporting Information, Figure S9). This observation supports the idea that upon light activation the excess membrane of the deflated GUVs contributes to the increase in adhesion area, whereas upon decrease in adhesion this membrane can spontaneously bud off. Yet, it should be noted that such loss of membrane over repeated light/dark cycles will be a limitation for motility over long distances. The budding may be an indication of a change in the membrane spontaneous curvature because of local asymmetry induced by protein interactions in the vicinity of the adhesion zone.[25]

For this study it was critical that there was a difference in binding strength in the dark and under blue light and that adhesion and detachment kinetics match, which led us to determine kinetic and thermodynamic parameters for the iLID and Micro interaction under blue light and in dark. In the QCM-D (quartz crystal microbalance with dissipation monitoring) studies, iLID was immobilized on a supported lipid bilayer (DOPC + 5 mol % DGS-NTA) formed on a SiO_2 crystal. Five mol % DGS-NTA was required in QCM-D measurements for the reliable detection of His-tagged iLID binding. Subsequently, increasing concentrations of Micro were passed over the QCM-D crystal either in the dark or under blue light illumination and both the binding and unbinding kinetics were monitored (Supporting Information, Figure S10). We observed that Micro binds to iLID both in the dark and under blue light, however the binding is more prominent under blue light. The analysis of the QCM-D curves showed that the K_d (dissociation constant) for the iLID− Micro interaction is 2.6 μM in the dark and 952 nM under
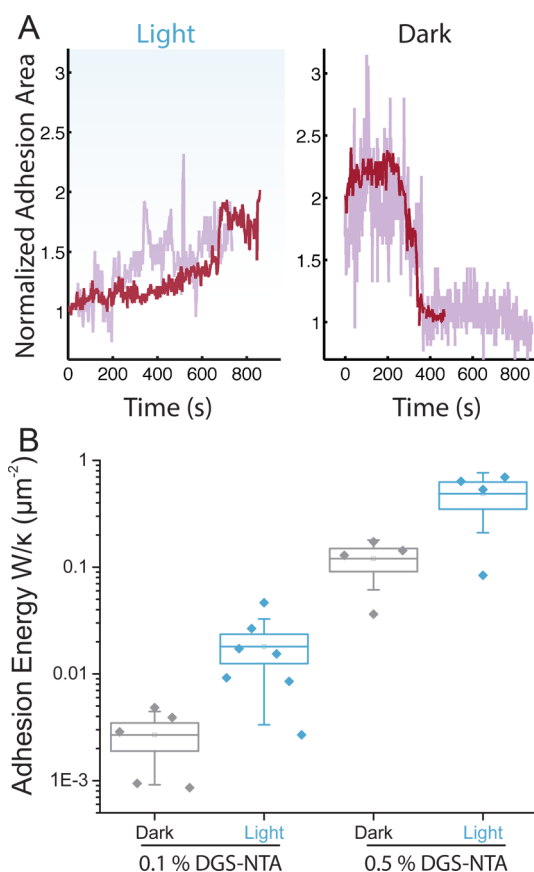
Figure 3. Quantification of adhesion. (A) Examples of time-dependent evolution of the normalized adhesion area versus time under blue light illumination and in the dark of two different GUVs (red and pink traces). Under blue light, an increase to about 1.8 times of the initial adhesion area was observed and subsequently in the dark the adhesion area decreased back to its initial value. Note that changes in adhesion area were related to adhesion energy, see eq 1 in SI. (B) Adhesion energies for GUVs functionalized with different Micro concentrations (0.1 mol % and 0.5 mol % DGS-NTA lipid for Micro immobilization) in the dark or under blue light. The adhesion energy W (rescaled by the GUV bending rigidity $\kappa \approx 20\ k_{\mathrm{B}}T$[28]) for the 0.1 mol % DGS-NTA containing GUVs under blue light activation corresponds to about $0.4\ k_{\mathrm{B}}T/\mu m^2$, which was used in the following light guiding experiments. All populations were found to be significantly different from each other ($p < 0.05$ Student t-test).

blue light, which equals a 2.7-fold increase in binding affinity under blue light (Supporting Information, Figure S11). Although a 2.7-fold difference in interactions seems small, it is notable that this difference is enough to trigger light-dependent adhesion of the GUVs. Further, these values are significantly different from the reported K_{d}s of 47 μM in the dark and 800 nM under blue light (58-fold change) of the proteins in solution,[22] showing that the immobilization of the iLID to a membrane affects the binding significantly. The k_{off} for the iLID−Micro interaction is similar in dark and under blue light ($k_{\mathrm{off,dark}} = 8.5 \times 10^{-4}$ s^{-1}, $k_{\mathrm{off,blue}} = 1.1 \times 10^{-3}$ s^{-1}) but the k_{on} increases significantly under blue light ($k_{\mathrm{on,dark}} = 3.2 \times 10^2$ M^{-1} s^{-1}, $k_{\mathrm{on,blue}} = 1.2 \times 10^3$ M^{-1} s^{-1}). These ranges of k_{off} and k_{on} are similar to those measured for integrin-extracellular protein binding (Supporting Information, Table S1).[26,27] This is an additional aspect in which the iLID-Micro interaction is similar to cell-matrix interactions of the cell in terms of

dynamics but without coupling them to the intracellular machinery.

The light-dependent adhesion of the GUVs was quantified by measurement of the membrane-substrate adhesion energy, which depends on the concentration of Micro on the GUV and number of light activated iLID on the substrate. In turn, the contact area and global shape of adhering GUVs depends on the adhesion energy, the membrane tension (or excess area) and the bending rigidity.[24] The osmotically deflated GUVs exhibited varying membrane tension and, as expected, areas of the adhered membrane segments were found to be heterogeneous within a population. To estimate the interaction energy between the GUV and substrate, the GUV area and volume were estimated from three-dimensional reconstructions obtained by confocal microscopy.[16,29] In the dark, when Micro surface concentration was kept low (0.1 mol % DGS-NTA lipid for anchoring His-tagged Micro to the GUV), the adhesion energies between GUV and substrate were found to be smaller than $10^{-1}\ k_{\mathrm{B}}T/\mu m^{-2}$ and GUVs were essentially unbound (Figure 3B left). In contrast, light activation increased the adhesion energy to about $0.4\ k_{\mathrm{B}}T/\mu m^{-2}$. The change of adhesion energy between the dark and blue light activated state is about 6-fold and, interestingly, exceeds the change in iLID-Micro binding affinity of 2.7 fold. Presumably, this effect is at least partly due to the cooperative and nonlinear dependence between membrane adhesion energy and receptor−ligand complex formation through suppression of membrane fluctuations.[30,31] As expected, an increase in Micro surface concentration (0.5 mol % DGS-NTA lipid, Figure 3B right) increased both adhesion energies in the dark- and light-activated state substantially but the adhesion energy remained higher under blue light. Notably, the GUVs with 0.5 mol % DGS-NTA lipid significantly adhered in the dark, which is not desired for the light-guided migration. It was not possible to increase the DGS-NTA lipid and hence the Micro concentration on the GUVs further because the GUVs with higher DGS-NTA lipid significantly aggregated. On the substrate side, if the iLID density was reduced by decreasing from 100% to 10% the PEG-NTA, the GUVs no longer adhered even under long blue light illumination (Supporting Information, Figure S12). Nonetheless, the adhesion energies between the GUVs and the substrate could be tuned over 3 orders of magnitude using the blue light-triggered interaction between iLID and Micro allowing for different applications. In the context of light guided motility, we used 0.1 mol % DGS-NTA lipid and 100% PEG-NTA to immobilize Micro on the GUVs and iLID on the substrate respectively, as this combination resulted in low adhesion in the dark and significant adhesion under blue light.

Even though cell motility is thoroughly studied, there are no minimal synthetic systems that are able to reproduce this behavior. A key feature of cell motility is the dynamic asymmetry in cell adhesions, which are forming at the leading edge and disassembling at the trailing edge as the cell moves forward. To mimic this dynamic asymmetry of adhesions in a synthetic minimal cell, we used light-controlled GUV adhesion. For this purpose, we observed the GUV (0.1 mol % DGS-NTA lipid) from below at the interface between the glass substrate and the GUV (x,y direction) on a confocal microscope to see the adhesion area of the GUV on the iLID functionalized substrate and locally illuminated half of the GUVs adhesion area as well as a free region in front of it (Figure 4A,B). The illumination led to spatiotemporally controlled imbalance in adhesions; more and new adhesions formed in the illuminated
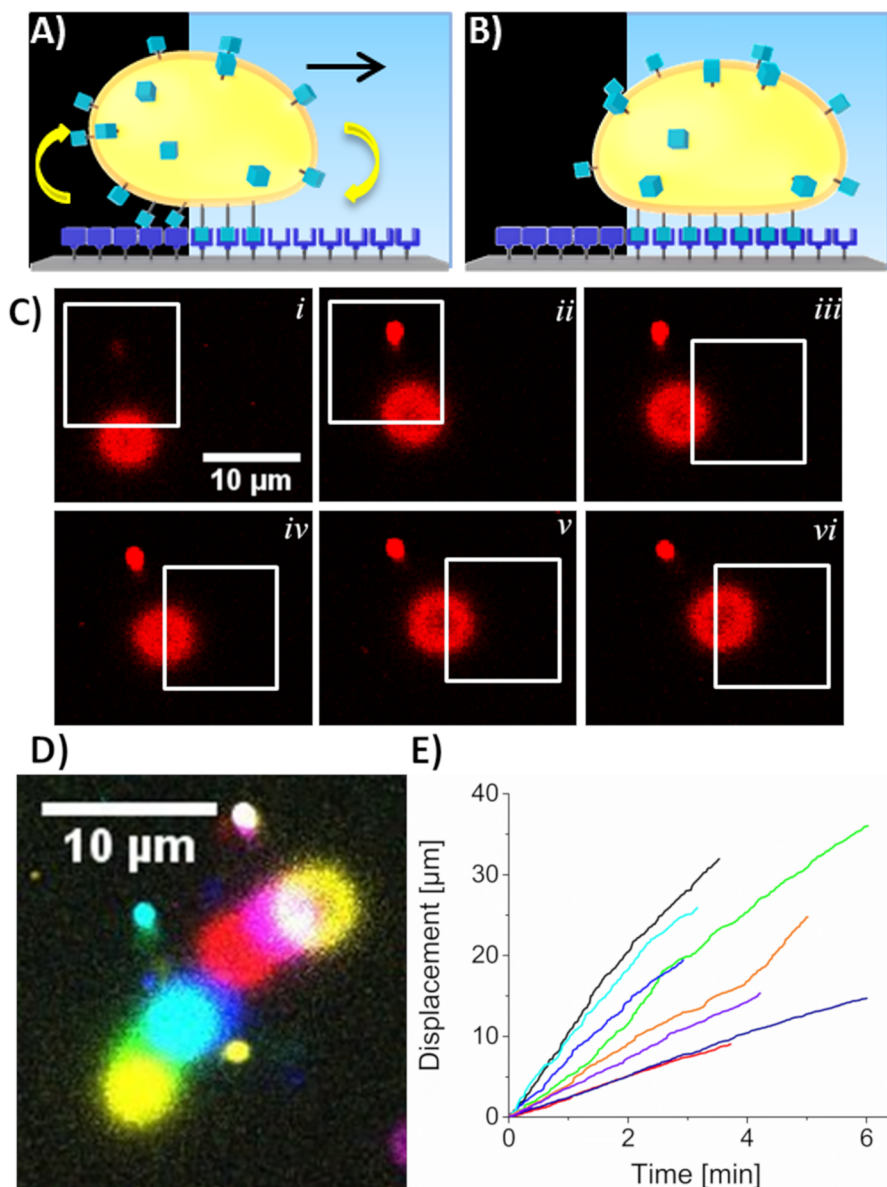
Figure 4. Light guiding. (A) Asymmetric illumination of the GUV leads to stronger adhesion in the illuminate area and weaker adhesion in the dark area. (B) This leads to migration of the GUV into the illuminated area. (C) Fluorescence microscopy images (x,y scans at the substrates surface $z = 0$) of a GUV (about 20 μm in diameter) from below at the adhesion site to the substrate as it moves into the blue illuminated area (shown as white square). (D) Overlay of the GUV at every illumination step (1 step about 1 min) to show GUV movement over time. (E) Displacement of GUVs versus time. Eight different GUV traces were analyzed.

half of the GUV compared to the half in the dark, where adhesions disassembled. Consequently, the GUV moved into the illuminated region, formed new adhesions in the illuminated area of the substrate, and detached from the dark part of the substrate (Figure 4 C,D, Supporting Information, Movie S1 and S2, Figure S13). Further, if the illuminated area was moved again so that only half of the GUV resides in it, the GUV followed and displaced into the new illumination area. This process could be repeated 3−7 times and the GUV could be guided over longer distances. This was also possible in multiple circuits like around a corner or back and forth (Supporting Information, Figures S14 and S15, Movie S3). In addition to the light-triggered asymmetry in adhesions, it was also essential to use deflated GUVs during light guided motility, so that the adhesion area of the GUV was large enough (about 5 μm radius) to be able to partially illuminate

the GUV and to create a significant imbalance in adhesions in space and time. Moreover, the fluctuations and excess membrane in the deflated GUV might be a compensation for protrusions observed during cell motility. During light guiding, we observed cases of visible membrane shedding and also a trail of membrane (Supporting Information, Figure S16). This loss of membrane is probably the reason why GUVs can be guided over only a couple of steps and not indefinitely. Although the speed of the GUVs depended on many factors including the size of the adhesion side, the GUV size, and the membrane tension, the average speed of eight representative GUVs was 4.9 μm/min (Figure 4E). This speed is reasonably fast and is comparable to a fast moving mammalian cell.[17]

Overall, we mimic cell motility in a minimal synthetic cell, assembled from molecular components. To achieve this, we dynamically and reversibly control the adhesion of a GUV to a

substrate in space and time using the light-dependent interaction between the proteins iLID and Micro. This makes it possible to guide the migration of a GUV with light by forming new adhesions at the front of a GUV through local illumination and disassembling adhesions at the back placed in the dark. The provided examples show that it is sufficient to reproduce the dynamic and spatiotemporally controlled asymmetry in adhesions between the front and the back of a migrating cell to move cell-sized objects. In the cell, this requires complex molecular machinery but in a minimal synthetic cell this can be achieved with photoswitchable adhesions.

■ ASSOCIATED CONTENT

ⓈSupporting Information

The Supporting Information is available free of charge on the ACS Publications website at DOI: 10.1021/acs.nano-lett.8b03469.

> Experimental methods, thermodynamic and kinetic characterization, controls and additional examples (PDF)
> Example of light-guided migration of the GUVs (AVI)
> Example of light-guided migration of the GUVs (AVI)
> Example of light-guided migration of the GUVs (AVI)

■ AUTHOR INFORMATION

Corresponding Author
*E-mail: wegners@mpip-mainz.mpg.de.
ORCID ⬡
Seraphine V. Wegner: 0000-0002-9072-0858

Author Contributions
S.M.B. and J.S. contributed equally.

Notes
The authors declare no competing financial interest.

■ REFERENCES

(1) Maiuri, P.; Rupprecht, J. F.; Wieser, S.; Ruprecht, V.; Benichou, O.; Carpi, N.; Coppey, M.; De Beco, S.; Gov, N.; Heisenberg, C. P.; Lage Crespo, C.; Lautenschlaeger, F.; Le Berre, M.; Lennon-Dumenil, A. M.; Raab, M.; Thiam, H. R.; Piel, M.; Sixt, M.; Voituriez, R. Actin flows mediate a universal coupling between cell speed and cell persistence. *Cell* **2015**, *161* (2), 374−86.

(2) Siton-Mendelson, O.; Bernheim-Groswasser, A. Toward the reconstitution of synthetic cell motility. *Cell Adh. Migr.* **2016**, *10* (5), 461−474.

(3) Smith, A. S.; Seifert, U. Vesicles as a model for controlled (de-)adhesion of cells: a thermodynamic approach. *Soft Matter* **2007**, *3* (3), 275−289.

(4) Fenz, S. F.; Sengupta, K. Giant vesicles as cell models. *Integr. Biol.* **2012**, *4* (9), 982−95.

(5) Tsai, F. C.; Stuhrmann, B.; Koenderink, G. H. Encapsulation of active cytoskeletal protein networks in cell-sized liposomes. *Langmuir* **2011**, *27* (16), 10061−71.

(6) Heuvingh, J.; Franco, M.; Chavrier, P.; Sykes, C. ARF1-mediated actin polymerization produces movement of artificial vesicles. *Proc. Natl. Acad. Sci. U. S. A.* **2007**, *104* (43), 16928−33.

(7) Hoesli, C. A.; Garnier, A.; Juneau, P. M.; Chevallier, P.; Duchesne, C.; Laroche, G. A fluorophore-tagged RGD peptide to control endothelial cell adhesion to micropatterned surfaces. *Biomaterials* **2014**, *35* (3), 879−90.

(8) Marchi-Artzner, V.; Lorz, B.; Gosse, C.; Jullien, L.; Merkel, R.; Kessler, H.; Sackmann, E. Adhesion of Arg-Gly-Asp (RGD) peptide vesicles onto an integrin surface: Visualization of the segregation of RGD ligands into the adhesion plaques by fluorescence. *Langmuir* **2003**, *19* (3), 835−841.

(9) Frohnmayer, J. P.; Bruggemann, D.; Eberhard, C.; Neubauer, S.; Mollenhauer, C.; Boehm, H.; Kessler, H.; Geiger, B.; Spatz, J. P. Minimal synthetic cells to study integrin-mediated adhesion. *Angew. Chem., Int. Ed.* **2015**, *54* (42), 12472−8.

(10) Gaul, V.; Lopez, S. G.; Lentz, B. R.; Moran, N.; Forster, R. J.; Keyes, T. E. The lateral diffusion and fibrinogen induced clustering of platelet integrin alphaIIbbeta3 reconstituted into physiologically mimetic GUVs. *Integr. Biol.* **2015**, *7* (4), 402−11.

(11) Streicher, P.; Nassoy, P.; Barmann, M.; Dif, A.; Marchi-Artzner, V.; Brochard-Wyart, F.; Spatz, J.; Bassereau, P. Integrin reconstituted in GUVs: a biomimetic system to study initial steps of cell spreading. *Biochim. Biophys. Acta, Biomembr.* **2009**, *1788* (10), 2291−300.

(12) Anamelechi, C. C.; Clermont, E. E.; Brown, M. A.; Truskey, G. A.; Reichert, W. M. Streptavidin binding and endothelial cell adhesion to biotinylated fibronectin. *Langmuir* **2007**, *23* (25), 12583−8.

(13) Fenz, S. F.; Merkel, R.; Sengupta, K. Diffusion and intermembrane distance: case study of avidin and E-cadherin mediated adhesion. *Langmuir* **2009**, *25* (2), 1074−85.

(14) Villringer, S.; Madl, J.; Sych, T.; Manner, C.; Imberty, A.; Romer, W. Lectin-mediated protocell crosslinking to mimic cell-cell junctions and adhesion. *Sci. Rep.* **2018**, *8* (1), 1932.

(15) Cardoso Dos Santos, M.; Vezy, C.; Jaffiol, R. Nanoscale characterization of vesicle adhesion by normalized total internal reflection fluorescence microscopy. *Biochim. Biophys. Acta, Biomembr.* **2016**, *1858* (6), 1244−53.

(16) Steinkuhler, J.; Agudo-Canalejo, J.; Lipowsky, R.; Dimova, R. Modulating Vesicle Adhesion by Electric Fields. *Biophys. J.* **2016**, *111* (7), 1454−1464.

(17) Maiuri, P.; Terriac, E.; Paul-Gilloteaux, P.; Vignaud, T.; McNally, K.; Onuffer, J.; Thorn, K.; Nguyen, P. A.; Georgoulia, N.; Soong, D.; Jayo, A.; Beil, N.; Beneke, J.; Lim, J. C.; Sim, C. P.; Chu, Y. S.; participants, W. C. R.; Jimenez-Dalmaroni, A.; Joanny, J. F.; Thiery, J. P.; Erfle, H.; Parsons, M.; Mitchison, T. J.; Lim, W. A.; Lennon-Dumenil, A. M.; Piel, M.; Thery, M. The first World Cell Race. *Curr. Biol.* **2012**, *22* (17), R673−5.

(18) Bartelt, S. M.; Chervyachkova, E.; Steinkuhler, J.; Ricken, J.; Wieneke, R.; Tampe, R.; Dimova, R.; Wegner, S. V. Dynamic blue light-switchable protein patterns on giant unilamellar vesicles. *Chem. Commun.* **2018**, *54* (8), 948−951.

(19) Zimmerman, S. P.; Hallett, R. A.; Bourke, A. M.; Bear, J. E.; Kennedy, M. J.; Kuhlman, B. Tuning the Binding Affinities and Reversion Kinetics of a Light Inducible Dimer Allows Control of Transmembrane Protein Localization. *Biochemistry* **2016**, *55* (37), 5264−71.

(20) Yüz, S. G.; Ricken, J.; Wegner, S. V. Independent Control over Multiple Cell Types in Space and Time Using Orthogonal Blue and Red Light Switchable Cell Interactions. *Adv. Sci.* **2018**, *5* (8), 1800446.

(21) Chen, F.; Wegner, S. V. Blue Light Switchable Bacterial Adhesion as a Key Step toward the Design of Biofilms. *ACS Synth. Biol.* **2017**, *6* (12), 2170−2174.

(22) Guntas, G.; Hallett, R. A.; Zimmerman, S. P.; Williams, T.; Yumerefendi, H.; Bear, J. E.; Kuhlman, B. Engineering an improved light-induced dimer (iLID) for controlling the localization and activity of signaling proteins. *Proc. Natl. Acad. Sci. U. S. A.* **2015**, *112* (1), 112−7.

(23) Schenk, F. C.; Boehm, H.; Spatz, J. P.; Wegner, S. V. Dual-functionalized nanostructured biointerfaces by click chemistry. *Langmuir* **2014**, *30* (23), 6897−905.

(24) Seifert, U.; Lipowsky, R. Adhesion of vesicles. *Phys. Rev. A: At., Mol., Opt. Phys.* **1990**, *42* (8), 4768−4771.

(25) Georgiev, V. N.; Grafmüller, A.; Bléger, D.; Hecht, S.; Kunstmann, S.; Barbirz, S.; Lipowsky, R.; Dimova, R. Area Increase and Budding in Giant Vesicles Triggered by Light: Behind the Scene. *Adv. Sci.* **2018**, *5* (8), 1800432.

(26) Hudson, S. V.; Dolin, C. E.; Poole, L. G.; Massey, V. L.; Wilkey, D.; Beier, J. I.; Merchant, M. L.; Frieboes, H. B.; Arteel, G. E. Modeling the Kinetics of Integrin Receptor Binding to Hepatic Extracellular Matrix Proteins. *Sci. Rep.* **2017**, *7*, 12444.

(27) Takagi, J.; Petre, B. M.; Walz, T.; Springer, T. A. Global conformational rearrangements in integrin extracellular domains in outside-in and inside-out signaling. *Cell* **2002**, *110* (5), 599−611.

(28) Dimova, R. Recent developments in the field of bending rigidity measurements on membranes. *Adv. Colloid Interface Sci.* **2014**, *208*, 225−34.

(29) Tordeux, C.; Fournier, J. B.; Galatola, P. Analytical characterization of adhering vesicles. *Phys. Rev. E: Stat. Phys., Plasmas, Fluids, Relat. Interdiscip. Top.* **2002**, *65*, 041912.

(30) Steinkuhler, J.; Rozycki, B.; Alvey, C.; Lipowsky, R.; Weikl, T. R.; Dimova, R.; Discher, D. E. Membrane fluctuations and acidosis regulate cooperative binding of "marker of self" CD47 with macrophage checkpoint receptor SIRPalpha. *J. Cell Sci.* **2019**, *4*, jcs216770.

(31) Weikl, T. R.; Asfaw, M.; Krobath, H.; Rózycki, B.; Lipowsky, R. Adhesion of membranes via receptor−ligand complexes: Domain formation, binding cooperativity, and active processes. *Soft Matter* **2009**, *5* (17), 3213.